Volume 17 | Number 2 | 14 January 2015 | Pages 185–472

CrystEngComm

www.rsc.org/crystengcomm

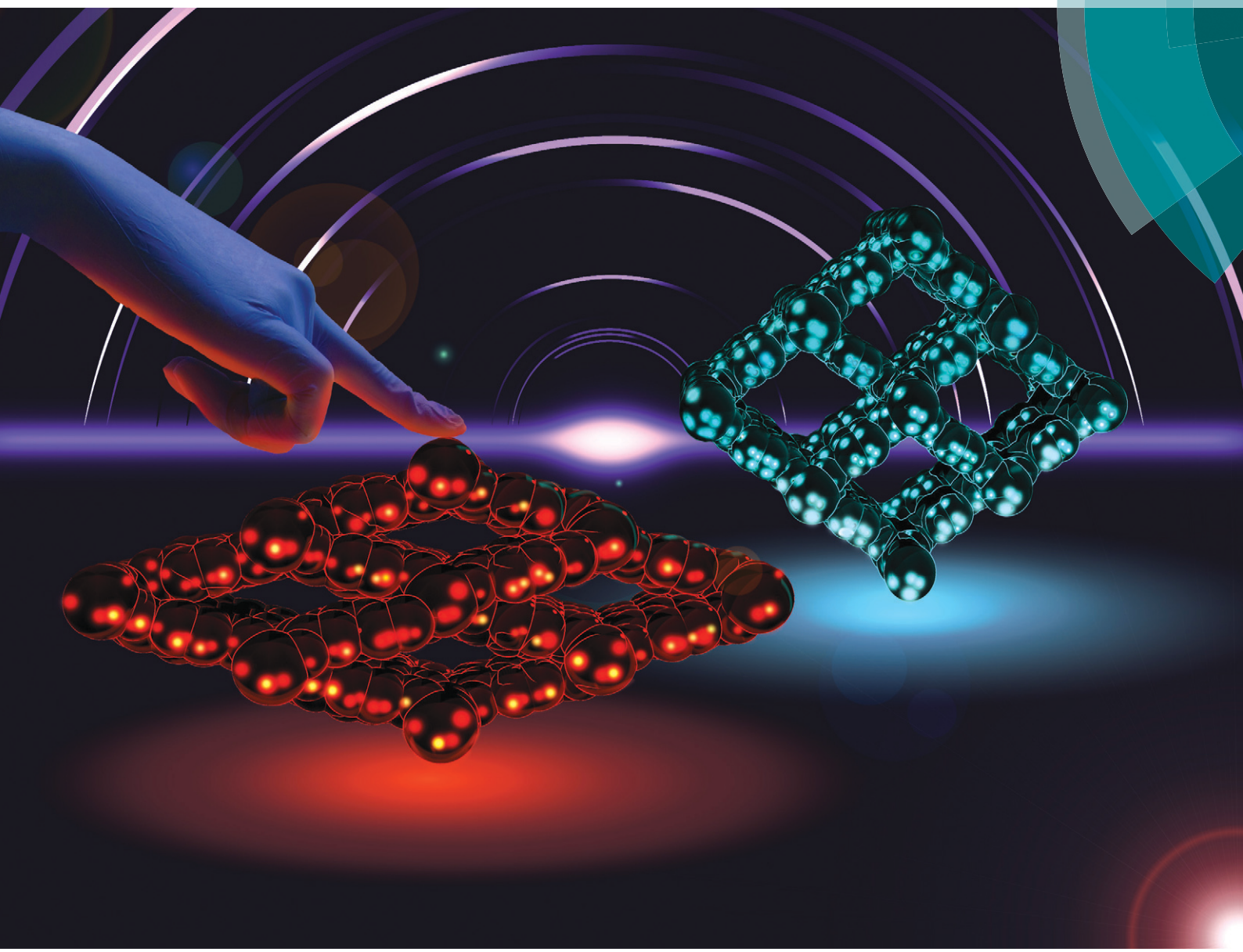

ROYAL SOCIETY OF CHEMISTRY

COMMUNICATION

Pablo Serra-Crespo, Jorge Gascon *et al.*

Experimental evidence of negative linear compressibility in the MIL-53 metal–organic framework family

CrystEngComm

COMMUNICATION

View Article Online
View Journal | View Issue

Cite this: *CrystEngComm*, 2015, **17**, 276

Received 3rd March 2014,
Accepted 24th March 2014

DOI: 10.1039/c4ce00436a

www.rsc.org/crystengcomm

Experimental evidence of negative linear compressibility in the MIL-53 metal–organic framework family†

Pablo Serra-Crespo,*[a] Alla Dikhtiarenko,[a] Eli Stavitski,[b] Jana Juan-Alcañiz,[a] Freek Kapteijn,[a] François-Xavier Coudert[c] and Jorge Gascon*[a]

We report a series of powder X-ray diffraction experiments performed on the soft porous crystals MIL-53(Al) and NH_2-MIL-53(Al) in a diamond anvil cell under different pressurization media. Systematic refinements of the obtained powder patterns demonstrate that these materials expand along a specific direction while undergoing total volume reduction under an increasing hydrostatic pressure. The results confirm for the first time the negative linear compressibility behaviour of this family of materials, recently predicted from quantum chemical calculations.

A special class of metal organic frameworks (MOFs) are those whose pore dimensions change upon external stimuli, the so-called soft porous crystals (SPCs).[1] In SPCs, adsorption and desorption of different molecules and changes in temperature or even mechanical pressure result in different phenomena like the breathing effect and the gate-opening effect, where pores contract or expand as a response.[2–4] One of the most studied SPCs is the MIL-53 family, built from $M(OH)_2$ octahedra (M being Fe^{3+}, Al^{3+}, Ga^{3+}, Cr^{3+}, In^{3+} or Sc^{3+}) and terephthalate ligands, resulting in one-dimensional pores with a diamond shape and unit cell changes from approximately 1500 Å^3 to 1000 Å^3.[5,6] The large difference in the pore volume is attributed to the so-called breathing effect. MIL-53(Al) is well known to undergo a phase transition from the large pore (lp) phase (pore volume of around 1500 Å^3) in the absence of an adsorbate to a narrow pore phase (pore volume of around 1000 Å^3) when exposed to certain molecules like water and carbon dioxide.[7] In the case of the amino functionalized version of MIL-53, the evacuated material shows a very narrow pore (vnp) phase in vacuum (pore volume *ca.* 940 Å^3). When exposed to different adsorbates, the NH2-MIL-53(Al) framework expands first to a narrow pore (np) phase (pore volume of around 990 Å^3) and then to a lp phase at higher adsorbate pressures (pore volume of approx. 1450 Å^3).[8]

As the interest in MOFs grew over the last two decades, several researchers have studied their thrilling mechanical properties: elastic behaviour, hardness, pressure-induced amorphization and pressure-induced structural transformations.[9–15] When it comes to SPCs, Beurroies *et al.* were able to induce the phase transition from the lp to the np configuration of MIL-53(Cr) by using external pressure.[16,17] More recently, we have reported the high amorphization resistance (>20 GPa) and high compressibility (K_0 = 10.9 GPa) of the NH_2-MIL-53(In) framework.[18] A combined computational and experimental work by Yot *et al.* demonstrated the agreement under mechanical pressure of the related material MIL-47, a vanadium-based MOF with the same topology as MIL-53 and for which adsorption- or temperature-induced breathing has never been observed.[19] In spite of these studies, there is still a major lack of experimental data on the fundamental mechanical properties of SPCs, especially when it comes to anisotropy of their elastic behaviour. While full tensorial studies of elasticity are starting to appear on some MOFs, including the measurement of ZIF-8's stiffness tensor by Brillouin scattering,[20] the few experimental studies on mechanical properties of SPCs so far only report the scalar bulk modulus. Indeed, these measurements fail to account for the *a priori* tensorial nature of compression and other important elastic properties of SPCs, like their Young's modulus, shear modulus, or Poisson's ratio, have not been experimentally investigated yet.

Only a limited number of solids expand along a specific direction while undergoing total volume reduction under an increasing mechanical pressure. This phenomenon is known as negative linear compressibility (NLC)[21] and has been

[a] *Catalysis Engineering, Technical University of Delft, Julianalaan 136, 2628 BL Delft, The Netherlands. E-mail: P.SerraCrespo@tudelft.nl, J.Gascon@tudelft.nl*
[b] *National Synchrotron Light Source, Brookhaven National Laboratory, Upton, NY, 11973, USA*
[c] *Institut de Recherche de Chimie Paris, CNRS – Chimie ParisTech, 11 rue Pierre et Marie Curie, 75005 Paris, France*

† Electronic supplementary information (ESI) available. See DOI: 10.1039/c4ce00436a

experimentally observed in some cyanide hybrid materials[22–24] and in a rigid zinc formate framework.[25] These materials share a common feature which gives rise to the NLC phenomenon: a wine-rack framework of the same topology as the framework of the MIL-53 family (see Fig. 1).[26]

Indeed, recent quantum chemical calculations have predicted that various MIL-53 materials, as well as other porous SPCs sharing this topology (such as MIL-47 and DMOF-1), should present very high NLC.[27,28] However, no experimental evidence of NLC on a SPC has been reported so far.

Herein, we report the NLC behaviour of MIL-53(Al) and NH_2-MIL-53(Al) (ref. 29–31) materials confirmed through a series of pressure-dependent powder X-ray diffraction experiments performed in a diamond anvil cell (DAC) under different pressurization liquid media.

MIL-53(Al) and NH_2-MIL-53(Al) were synthesized and activated according to the literature.[7,32] The experiments were performed using synchrotron radiation at the beamline X17C of the National Synchrotron Light Source (NSLS). The DAC consists of two opposing diamonds with a sample chamber created between both culets. In order to avoid axial tensions, a 0.25 mm pre-indented gasket is placed in between the culets and filled with a fluid used to apply a hydrostatic pressure.[33] The pressure inside the chamber is monitored by observation of the fluorescence of a small ruby chip placed inside the chamber. The position of the fluorescence band of this material has a linear dependence in the region from 0 to 25 GPa.[34] Prior to the insertion into the chamber, the sample was activated and compacted. After that, the chamber was loaded with the pressurization liquid and then the pressure was increased step by step. Pressure was measured before and after the experiments and no differences were found.

The X-ray powder diffraction patterns at different pressures were fitted to the simulated patterns calculated on the basis of the published structures.[7,29] The initial structure models for cell refinements were constructed from unit cell parameters taken from previously reported MIL-53(Al) (ref. 7) and NH_2-MIL-53(Al) in lp and np forms.[29] The resulting pressure-dependent lattice parameters were obtained by Rietveld refinement, performed on the pressure-applied data using the WinPLOTR and FullProf software.[35,36] A pseudo-Voigt function was chosen to generate the line shape of the diffraction peaks. First, the zero offset, the scale factor, twelve background terms, profile parameters and the unit cell were refined. The studied materials considered amorphous and lead to unreasonable pattern matching when the diffraction peaks became broad and their intensities were less than 5.0% of the background level, complying 8 FWHT range for calculation of single reflection.

In Fig. 2 the changes in volume and cell parameters of MIL-53(Al) are presented as a function of the applied pressure, using mineral oil as pressure-transmitting medium (lattice parameter data of the pressure dependent experiments with mineral oil and ethanol as pressure media on MIL-53(Al) can be found in Table S1 and S2,† respectively). Despite the fact that only few data points could be collected, important information can be extracted from these results. In the first place, the material is crystalline up to 6 GPa, on the same order of magnitude as the most pressure resistant MOFs.[37]

When focusing on the evolution of the different cell parameters (Table S1†), two successive regimes can be observed. First, upon increasing pressure from 0 to 3 GPa, the material expands in the *b* direction while contracting in the *a* and *c* directions, demonstrating NLC in one direction. The linear compressibilities calculated in this range are β_a = 23 TPa^{-1}, β_b = −28 TPa^{-1} and β_c = 59 TPa^{-1}. The negative value along the *b* axis is much larger than those measured in other metal–organic frameworks, −4.32 TPa^{-1} for Ag(mim) (ref. 26) and −1.8 TPa^{-1} for $[NH_4][Zn(HCOO)_3]$,[25] demonstrating the very large NLC character of MIL-53(Al) in this pressure range. This large value of β_b, obtained in a wide pressure range, is as expected smaller than the value calculated by quantum chemical calculations in the elastic regime, which corresponds to infinitesimal deformations (*i.e.* the limit of $P \rightarrow 0$). Then, at higher pressure ($P \geq 3$ GPa), the overall pressure-induced contraction dominates the behaviour of MIL-53(Al), showing positive linear compressibility along all axes.

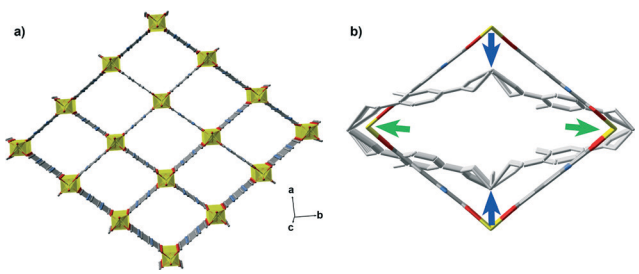

Fig. 1 (a) The MIL-53 framework in its lp configuration, with a wine-rack framework topology and (b) the expected NLC behaviour.

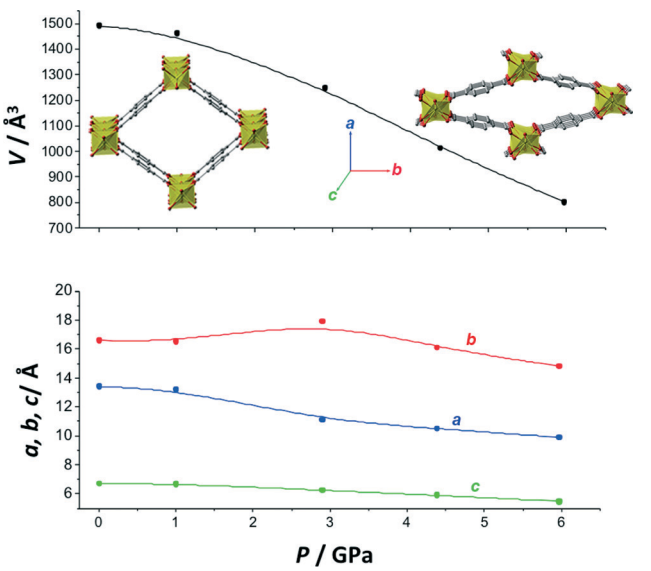

Fig. 2 Evolution of the cell volume (top) and lattice parameters (bottom) of MIL-53(Al) with increasing hydrostatic pressure using mineral oil as pressurization medium. The lattice parameters are shown in blue (*a*), red (*b*) and green (*c*). Lines are only for guidance.

Similar experiments performed on the functionalized NH_2-MIL-53(Al) are shown in Fig. 3. The change in the cell volume is displayed for the two different pressure media (the lattice parameters for both series of experiments can be found in Table S3 and S4† with mineral oil and ethanol as pressure media, respectively). When using mineral oil, two different regions can be observed: (i) from 0 up to 2 GPa and (ii) from 2 to above 11 GPa, where the material becomes amorphous. In the first region, the cell volume is decreased from 1433 $Å^3$ to around 1000 $Å^3$, matching the change in the volume corresponding to the lp to np transition. The fact that the starting cell volume is 1433 $Å^3$ indicates that the mineral oil penetrates into the pores (in the absence of the adsorbate NH_2-MIL-53(Al) displays a smaller cell volume), something that could not be concluded in the case of MIL-53(Al).

Results obtained using smaller fluid molecules such as ethanol are less conclusive, since densely packed ethanol in the pores leads to the formation of a denser phase that does not undergo the well-known lp to np transition. A clear lp–np transition is observed with increasing pressure, attributed to the lower affinity of mineral oil compared with ethanol and to the partial penetration at the starting pressure. With increasing pressure the oil is squeezed out of the sample. Two different bulk moduli were calculated for the two different regions, 7.4 GPa for the pressure range 0 to 2 GPa and 71 GPa for 2 to 11 GPa. The first value is in line with very soft materials and is in agreement with such a change in the volume. In the second region the material behaves like a dense phase, in very good agreement with the bulk modulus obtained, 85 GPa, using ethanol as the compressing fluid in the whole pressure range.[9]

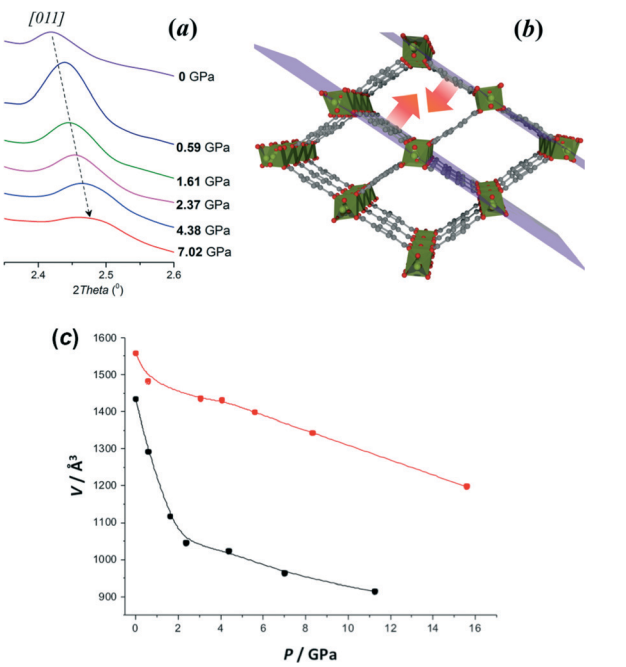

Fig. 3 (a) Displacement of the peak corresponding to the [011] plane as a function of the applied pressure on NH_2-MIL-53(Al) using mineral oil as pressurization medium. (b) The graphical representation of the NH_2-MIL-53(Al) structure showing the decreasing interplanar distance upon pressurization. (c) Evolution of the cell volume with increasing hydrostatic pressure using ethanol (red) and mineral oil (black). Lines are only for guidance.

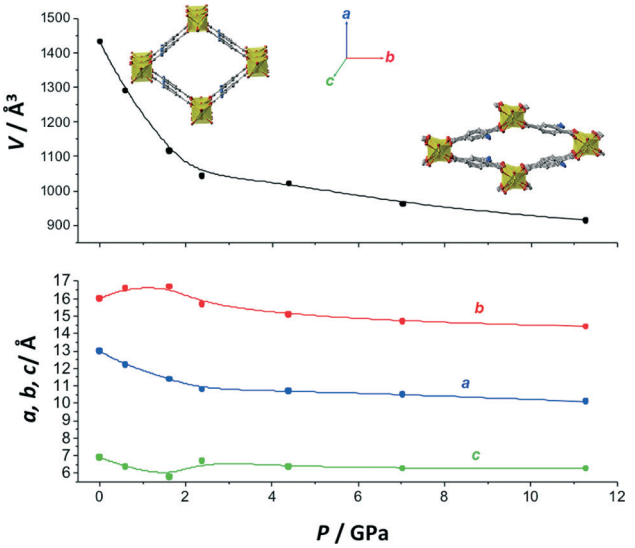

Fig. 4 Evolution of the cell volume (top) and lattice parameters (bottom) of NH_2-MIL-53(Al) with increasing hydrostatic pressure using mineral oil as pressurization medium. The lattice parameters are shown in blue (*a*), red (*b*) and green (*c*). Lines are only for guidance.

Finally, the evolution of the lattice parameters of NH_2-MIL-53(Al) with pressure was studied using mineral oil as the hydrostatic fluid, as depicted in Fig. 4. As is the case for MIL-53(Al), the NH_2-MIL-53(Al) framework shows an expansion in the *b* direction along with a contraction in the *a* direction at pressures up to 2 GPa. These observations are completely consistent with the gradual shifting of the diffraction peak at *ca.* 4.45°, corresponding to the [011] plane, to higher angles (Fig. 3). The values of the linear compressibility in this region are β_a = 99 TPa^{-1}, β_b = −27 TPa^{-1} and β_c = 76 TPa^{-1}, demonstrating not only anisotropy but also a high degree of NLC as a generic feature of this family of materials. To understand the mechanism that leads to the NLC phenomenon in MIL-53(Al) and NH2-MIL-53(Al), the stiff structural inorganic Al(OH) chains can be visualized to act as spindles in the flexible framework that behave as hinges (or centers of flexibility). Dicarboxylate linkers in the orthogonal plane connect these spindles to each other, acting as rigid struts. The rigidity of the struts in this wine-rack geometry enforces a connection between variations in the *a* and *b* lattice parameters: when *a* decreases, *b* increases (in the linear elastic regime, see Fig. 3b). This gives rise to the NLC phenomenon.

Conclusions

Refinement of powder X-ray diffraction data collected in a diamond anvil cell and different pressurization media from MIL-53(Al) and NH_2-MIL-53(Al) shows high pressure

resistance and the highest negative linear compressibility of this family of SPCs. This provides experimental confirmation of the negative linear compressibility of these materials, recently predicted on the basis of quantum chemistry calculations. The pressure needed to amorphize these materials was between 5 and 16 GPa for the studied media, ethanol and mineral oil. We attribute the high amorphization resistance to the NLC behaviour of these SPCs, allowing bonds to relax upon pressurization. These results are of utmost importance not only for shaping these MOFs, where the large anisotropy of their mechanical behaviour and NLC might pose some difficulties, but also for matching the mechanical properties of SPCs with other materials for the processing of composites, *e.g.* together with polymers for applications as membranes or in optoelectronics.[38,39]

Acknowledgements

We are grateful to Zhiqiang Chen for his help with XRD experiments. This research was partially supported by COMPRES, the Consortium for Materials Properties Research in Earth Sciences, under NSF Cooperative Agreement EAR 10-43050. Use of the National Synchrotron Light Source, Brookhaven National Laboratory, was supported by the U.S. Department of Energy, Office of Science, Office of Basic Energy Sciences, under contract no. DE-AC02-98CH10886. The research leading to these results has received funding from the European Research Council under the European Union's Seventh Framework Programme (FP/2007-2013)/ERC grant agreement no. 335746, CrystEng-MOF-MMM.

Notes and references

1 S. Horike, S. Shimomura and S. Kitagawa, *Nat. Chem.*, 2009, **1**, 695–704.
2 G. Férey and C. Serre, *Chem. Soc. Rev.*, 2009, **38**, 1380–1399.
3 C. Serre, C. Mellot-Draznieks, S. Surble, N. Audebrand, Y. Filinchuk and G. Férey, *Science*, 2007, **315**, 1828–1831.
4 J. van den Bergh, C. Gücüyener, E. A. Pidko, E. J. M. Hensen, J. Gascon and F. Kapteijn, *Chem. – Eur. J.*, 2011, **17**, 8832–8840.
5 F. Millange, C. Serre and G. Férey, *Chem. Commun.*, 2002, 822–823.
6 C. Serre, F. Millange, C. Thouvenot, M. Nogues, G. Marsolier, D. Louer and G. Férey, *J. Am. Chem. Soc.*, 2002, **124**, 13519–13526.
7 T. Loiseau, C. Serre, C. Huguenard, G. Fink, F. Taulelle, M. Henry, T. Bataille and G. Férey, *Chem. – Eur. J.*, 2004, **10**, 1373–1382.
8 S. Couck, E. Gobechiya, C. E. A. Kirschhock, P. Serra-Crespo, J. Juan-Alcañiz, A. Martinez Joaristi, E. Stavitski, J. Gascon, F. Kapteijn, G. V. Baron and J. F. M. Denayer, *ChemSusChem*, 2012, 740–750.
9 J. C. Tan and A. K. Cheetham, *Chem. Soc. Rev.*, 2011, **40**, 1059–1080.
10 K. W. Chapman, G. J. Halder and P. J. Chupas, *J. Am. Chem. Soc.*, 2008, **130**, 10524–10526.
11 E. C. Spencer, R. J. Angel, N. L. Ross, B. E. Hanson and J. A. K. Howard, *J. Am. Chem. Soc.*, 2009, **131**, 4022–4026.
12 K. W. Chapman, G. J. Halder and P. J. Chupas, *J. Am. Chem. Soc.*, 2009, **131**, 17546–17547.
13 S. A. Moggach, T. D. Bennett and A. K. Cheetham, *Angew. Chem., Int. Ed.*, 2009, **48**, 7087–7089.
14 K. J. Gagnon, C. M. Beavers and A. Clearfield, *J. Am. Chem. Soc.*, 2013, **135**, 1252–1255.
15 A. U. Ortiz, A. Boutin, A. H. Fuchs and F.-X. Coudert, *J. Phys. Chem. Lett.*, 2013, **4**, 1861–1865.
16 I. Beurroies, M. Boulhout, P. L. Llewellyn, B. Kuchta, G. Férey, C. Serre and R. Denoyel, *Angew. Chem., Int. Ed.*, 2010, **49**, 7526–7529.
17 A. V. Neimark, F. X. Coudert, C. Triguero, A. Boutin, A. H. Fuchs, I. Beurroies and R. Denoyel, *Langmuir*, 2011, **27**, 4734–4741.
18 P. Serra-Crespo, E. Stavitski, F. Kapteijn and J. Gascon, *RSC Adv.*, 2012, **2**, 5051–5053.
19 P. G. Yot, Q. Ma, J. Haines, Q. Yang, A. Ghoufi, T. Devic, C. Serre, V. Dmitriev, G. Férey, C. Zhong and G. Maurin, *Chem. Sci.*, 2012, **3**, 1100.
20 J.-C. Tan, B. Civalleri, C.-C. Lin, L. Valenzano, R. Galvelis, P.-F. Chen, T. D. Bennett, C. Mellot-Draznieks, C. M. Zicovich-Wilson and A. K. Cheetham, *Phys. Rev. Lett.*, 2012, 108.
21 R. H. Baughman, S. Stafström, C. Cui and S. O. Dantas, *Science*, 1998, **279**, 1522–1524.
22 A. B. Cairns, J. Catafesta, C. Levelut, J. Rouquette, A. van der Lee, L. Peters, A. L. Thompson, V. Dmitriev, J. Haines and A. L. Goodwin, *Nat. Mater.*, 2013, **12**, 212–216.
23 A. B. Cairns, A. L. Thompson, M. G. Tucker, J. Haines and A. L. Goodwin, *J. Am. Chem. Soc.*, 2011, **134**, 4454–4456.
24 A. L. Goodwin, D. A. Keen and M. G. Tucker, *Proc. Natl. Acad. Sci. U. S. A.*, 2008, **105**, 18708–18713.
25 W. Li, M. R. Probert, M. Kosa, T. D. Bennett, A. Thirumurugan, R. P. Burwood, M. Parinello, J. A. K. Howard and A. K. Cheetham, *J. Am. Chem. Soc.*, 2012, **134**, 11940–11943.
26 J. M. Ogborn, I. E. Collings, S. A. Moggach, A. L. Thompson and A. L. Goodwin, *Chem. Sci.*, 2012, **3**, 3011.
27 A. U. Ortiz, A. Boutin, A. H. Fuchs and F.-X. Coudert, *Phys. Rev. Lett.*, 2012, **109**, 195502.
28 A. U. Ortiz, A. Boutin, A. H. Fuchs and F.-X. Coudert, *J. Chem. Phys.*, 2013, **138**, 174703–174708.
29 S. Couck, E. Gobechiya, C. E. A. Kirschhock, P. Serra-Crespo, J. Juan-Alcañiz, A. Martinez Joaristi, E. Stavitski, J. Gascon, F. Kapteijn, G. V. Baron and J. F. M. Denayer, *ChemSusChem*, 2012, **5**, 740–750.
30 P. Serra-Crespo, M. A. van der Veen, E. Gobechiya, K. Houthoofd, Y. Filinchuk, C. E. A. Kirschhock, J. A. Martens, B. F. Sels, D. E. De Vos, F. Kapteijn and J. Gascon, *J. Am. Chem. Soc.*, 2012, **134**, 8314–8317.
31 E. Stavitski, M. Goesten, J. Juan-Alcañiz, A. Martinez-Joaristi, P. Serra-Crespo, A. V. Petukhov, J. Gascon and F. Kapteijn, *Angew. Chem.*, 2011, **123**, 9798–9802.
32 P. Serra-Crespo, E. Gobechiya, E. V. Ramos-Fernandez, J. Juan-Alcañiz, A. Martinez-Joaristi, E. Stavitski, C. E. A. Kirschhock,

J. A. Martens, F. Kapteijn and J. Gascon, *Langmuir*, 2012, **28**, 12916–12922.
33 A. Katrusiak, *Acta Crystallogr., Sect. A: Found. Crystallogr.*, 2008, **64**, 135–148.
34 R. A. Forman, G. J. Piermarini, J. Dean Barnett and S. Block, *Science*, 1972, **176**, 284–285.
35 T. Roisnel and J. Rodríguez-Carvajal, *WinPLOTR: A windows tool for powder diffraction pattern analysis*, 2001, vol. 378–381, pp. 118–123.
36 J. Rodríguez-Carvajal, *Phys. B*, 1993, **192**, 55–69.
37 Y. H. Hu and L. Zhang, *Phys. Rev. B: Condens. Matter Mater. Phys.*, 2010, **81**, 174103.
38 T. Rodenas, M. van Dalen, E. García-Pérez, P. Serra-Crespo, B. Zornoza, F. Kapteijn and J. Gascon, *Adv. Funct. Mater.*, 2014, **24**, 249–256.
39 T. Rodenas, M. van Dalen, P. Serra-Crespo, F. Kapteijn and J. Gascon, *Microporous Mesoporous Mater.*, 2013, DOI: 10.1016/j.micromeso.2013.08.049.